Characterizing Water Soluble Organic Carbon and their Effect on Cloud Droplet Formation

Carbonaceous aerosols constitute a significant fraction of atmospheric particulate matter. Water Soluble Organic Compounds (WSOC) can be a major component of the aerosol distribution and have been previously shown to noticeably affect key parameters that govern cloud droplet formation. Our primary focus has been to study the activation properties of cloud condensation nuclei (CCN) that contain WSOC to generate a database of thermo-physical properties that can be incorporated within aerosol-cloud interaction parameterizations. Investigation into WSOC CCN activation, growth kinetics and surface active properties will provide a more detailed perspective on organic aerosol cloud droplet formation and will thus improve the current understanding of climate change and prediction. During the past three years of this proposal, organics from a varied range of sources have been studied; laboratory generated and ambient aerosol characteristic of biomass burning, marine, urban and secondary organic aerosol (SOA) sources have been characterized. This review summarizes the initial proposal goals and highlights the completed and insightful objectives of the project.

Introduction

Aerosols have the ability to significantly change climate directly by scattering or absorbing light or indirectly via their interactions with clouds. Carbonaceous compounds can comprise 20-70% of the total aerosol mass [1-3] and thus are of importance to the understanding and prediction of climate change. Specifically, water soluble organic compounds (WSOC) may attribute 10-70% of the total organic fraction and their characteristics can significantly affect the ability of these aerosols, or cloud condensation nuclei (CCN), to interact with water vapor and form cloud. Studies have shown that WSOC can influence CCN hygroscopicity, surface tension, and possibly, droplet growth kinetics [4-6], properties all central to assessing the aerosol-indirect effect.

This proposal aims to improve our understanding of the aerosol indirect effect of carbonaceous aerosol, and is composed of an experimental and modeling component. The experimental component consists of laboratory and field studies of cloud condensation nuclei (CCN) that contain a significant fraction of organic material, using novel techniques developed during this proposal, that allow to quantitatively determine the impact of organics on surface tension, solute, and the growth rate of droplets. These quantitative impacts are expressed in terms of average organic thermodynamic properties (such as molar volume, solubility and surface tension depression, and water vapor uptake coefficient). The derived organic properties are then to be used in state-of-the art aerosol-cloud interactions modules developed by the PI and his research group (Nenes and Seinfeld, 2003; Fountoukis and Nenes, 2005; Barahona and Nenes, 2007), currently integrated within the NASA GISS GCM and the NASA Global Modeling Initiative frameworks. The augmented global climate model is then used to assess the aerosol indirect effect of carbonaceous aerosol. The following objectives have been identified in the original proposal:

Objective 1. Development of a novel CCN measurement method, that allows the inference of aggregate thermodynamic properties of the carbonaceous aerosol. Evaluation of the novel CCN measurement method with laboratory experiments of CCN activation

Objective 2: Laboratory/Field experiments of CCN activation, focusing on the properties of carbonaceous aerosol

All the objectives have been accomplished. In addition to the above, a number of new exciting research opportunities appeared that we have pursued and acknowledged support through this NASA/ESSF proposal. Details are given in the following sections.

Objective 1: Continued Development of the novel CCN measurement methods

We have continued developing the Scanning Mobility CCN Analysis (SMCA) methodology originally proposed, and now have submitted the methodology for publication (Nenes and Medina, Aerosol Science and Technology, *in review*). SMCA is now the method of choice to obtaining size-resolved CCN measurements, as it allows for a very fast characterization of the CCN activity and growth kinetics; this is particularly useful for systems that vary over time, and, also for characterizing the CCN properties of organic matter, for which limited sample is available.

This year we have further developed "Köhler theory analysis" (KTA) (Padró et al., 2008; Asa-Awuku et al., 2008), a method developed during this proposal, that uses size-resolved CCN measurements, combined with measurements of chemical composition of the inorganic fraction for constraining the thermodynamic properties (molar volume, surface tension depression), as well as impact on droplet growth kinetics of the organic component of the aerosol.

Milestone: Evaluation of the ability of Köhler theory analysis to concurrently infer the molar volume and surface tension impacts of organics in aerosol.

Knowing the surface tension of droplets at their point of activation is required for predicting their CCN activity. Unfortunately, direct measurement of σ of water-soluble organic carbon (WSOC) solutions at concentrations relevant for CCN activation (10^3 ppm and above) requires significant amount of mass (10^3 μg and above) or usage of dilute WSOC sample. If the latter is used, extrapolation of surface tension depression measurements to higher concentrations of WSOC is subject to substantial uncertainty. For this, we have developed an alternate method of inferring σ from CCN measurements, as described in the 2006-2007 report. This year, we have evaluated the method and shown that it successfully retrieves the molar volume and surface tension depression for complex water-soluble organic matter, such as dissolved marine organic matter, and, secondary organic aerosol. Examples of this method are provided in the Objective 2 studies.

Objective 2: Laboratory/Field experiments of CCN activation

CCN PROPERTIES OF BIOMASS BURNING AEROSOL

A major source of WSOC is from biomass burning. In pyrogenic air masses, WSOC can account for 45-75% of the total carbon aerosol mass [7]. The resulting compounds may be characterized as humic-like substances (HULIS), primarily carboxylic acids, and in aerosol samples can account for 60% of the WSOC [8]. HULIS are high molecular weight hydrophobic compounds that have been shown to act as strong surfactants [9]. HULIS are highly prevalent in continental aerosol, and have been isolated in urban, rural and smog samples [8-13]. Its prevalence suggests that properties attributed to HULIS are representative of a significant fraction of carbonaceous material found in nature. Surface-active properties can be enhanced in the presence of salts, in particular $(NH_4)_2SO_4$ [8] and hence the effect of surface active properties must be accounted for in cloud microphysical observations and calculations.

The CCN activity of the water-soluble organics in biomass burning aerosol was studied. The aerosol, after collection upon filters during a controlled biomass burning event, was dissolved in water using sonication. Hydrophobic and hydrophilic components were fractionated from a portion of the original sample using solid phase extraction, and subsequently desalted. The surface tension and CCN activity of these different samples were measured and the measurements show that the strongest surfactants are isolated in the hydrophobic fraction, while the hydrophilics exhibit negligible surface tension depression. The presence of salts (primarily $(NH4)2SO4$) in the hydrophobic fraction substantially enhances surface tension depression; their synergistic effects considerably enhance CCN activity, exceeding that of pure $(NH4)2SO4$. From our analysis, average thermodynamic properties (i.e, molar volume) are determined for samples using the Köhler Theory Analysis (KTA) method (also developed during this study). The molar mass of the hydrophilic and hydrophobic aerosol components is estimated to be 87±26 g mol^{-1} and 780±231 g mol^{-1}, respectively. KTA also suggests that the relative proportion (in moles) of hydrophobic to hydrophilic compounds in the original sample to be 1:3. For the first time, KTA was applied to an aerosol with a significant level of complexity and displays its potential for providing physically-based constraints for GCM parameterizations of the aerosol indirect effect. The results from this work have been published in:

Asa-Awuku, A., Nenes, A., Sullivan, A.P., Hennigan, C.J. and Weber, R.J. (2008) Investigation of molar volume and surfactant characteristics of water-soluble organic compounds in biomass burning aerosol, Atmos. Chem. Phys., 8, 799-812

THERMODYNAMIC PROPERTIES OF SECONDARY ORGANIC AEROSOL

Aerosol WSOC can either be emitted as primary organic aerosol or formed in the atmosphere through secondary oxidation of volatile organic carbon (VOC) to yield secondary organic aerosol (SOA). Natural VOC emissions (e.g., monoterpernes, sesquiterpenes), the major source of SOA, are estimated to be on the order of 1150 Tg yr^{-1} [14], and are thought to rival anthropogenic emissions [15-17]. Consequentially, studies suggest that the SOA fraction can contribute significantly to the total organic particulate mass, at least 50% of the primary organic aerosol emissions [17, 18], and hence could potentially be a significant source of WSOC.

SOA can be formed in reactions of biogenic hydrocarbons with OH, NO_3 and O_3 [17, 19-31]. Several studies use chemical speciation methods (i.e., mass spectrometry) [20, 23, 24, 27, 28] to characterize SOA, but 80 to 90% [27, 32, 33] of the chemical identity of all organic mass remains unknown. As a consequence, the thermodynamic properties of aggregate organic aerosol properties necessary to constrain cloud droplet formation have remained elusive [17].

For this proposal, the CCN properties, surfactant characteristics, and droplet growth kinetics of SOA formed from the ozonolysis of monoterpene, sesquiterpene and three parent alkene hydrocarbons (terpinolene, 1-methlycycloheptene and cycloheptene) were explored. The results and findings have been submitted and the CCN activity of monoterpene SOA has been published. The results from all three papers suggest that the water-soluble organics in the SOA are composed of relatively low molecular weight species, with an effective molar mass less than 200 g mol^{-1}. This finding was consistent with the speciated fraction for some of the SOA, and suggests that KTA can be applied to complex organic aerosol, such as that found in the atmosphere. The results are cited as follows:

Asa-Awuku, A., A. Nenes, S. Gao, R.C.Flagan, and J.H. Seinfeld, Alkene ozonolysis SOA: inferences of composition and droplet growth kinetics from Kohler theory analysis, Atmos. Chem. Phys. Discuss., in review

Asa-Awuku, A., Engelhart, G.J., Lee, B.H., Pandis, S.N., and Nenes, A., Relating CCN activity, volatility, and droplet growth kinetics of beta-caryophyllene secondary organic aerosol, Atmos. Chem. Phys. Discuss., in review

Engelhart, G.J., Asa-Awuku, A., Nenes, A., and Pandis, S.N., CCN activity and droplet growth kinetics of fresh and aged monoterpene secondary organic aerosol, Atmos. Chem. Phys., 8, 3937-3949

Particularly interesting has been the study on linking CCN activity with SOA volatility, composition and droplet growth kinetics for β-caryophyllene SOA. We further develop it below.

Relating CCN activity, volatility, and droplet growth kinetics of β-caryophyllene secondary organic aerosol.

In this study we investigate the droplet formation characteristics of aging β-caryophyllene secondary organic aerosol (SOA) generated via seedless dark ozonolysis. Employing two different CCN counters, we comprehensively characterize the CCN activity and droplet kinetics of the SOA, and explore the role of its volatile fraction on droplet formation. From filter samples of SOA obtained during these experiments, surfactant characteristics, average molar volume and droplet growth kinetics of the water-soluble component are determined with KTA. SOA and water-soluble organic carbon measurements are then combined to infer the soluble fraction of SOA, as well as the impacts of chemical aging thereon. Finally, we explore the

impact of composition (i.e., insoluble fraction) on droplet growth kinetics, by combining the CCN activation measurements with comprehensive models of the CCN instrumentation.

Samples, Experimental Description and Analysis Overview

Experiments in this study were conducted in the Carnegie Mellon University 12 m^3 Teflon SOA chamber suspended inside a temperature-controlled room. The aerosol generated in the chamber inlet is classified by a scanning mobility particle sizer (SMPS 3080) and differential mobility analyzer (DMA 3081). The total aerosol concentration (CN) of the monodisperse particles is counted by a condensation particle counter (TSI CPC 3010) and the CCN concentration is measured by a DH Associates-M1 Static Diffusion (SD) CCN Counter and a DMT Continuous-Flow Streamwise Thermal Gradient CCN Counter (CFSTGC). The SOA was formed in unseeded dark ozonolysis of β-caryophyllene. For each dry chamber experiment, oxidation occurred at 22°C at low relative humidity (3-8%); aerosol measurements commenced after the injection of sesquiterpene and lasted up to 11 hours. In some experiments, 0.5 ml of 2-butanol was used as hydroxyl radical (OH) scavenger so oxidation could occur in the presence and absence of OH. The SOA was at times passed through a thermodenuder (TD) at 35°C (close to the conditions found in the CFSTGC) for ~15 seconds before introduction to aerosol classification and CCN measurements.

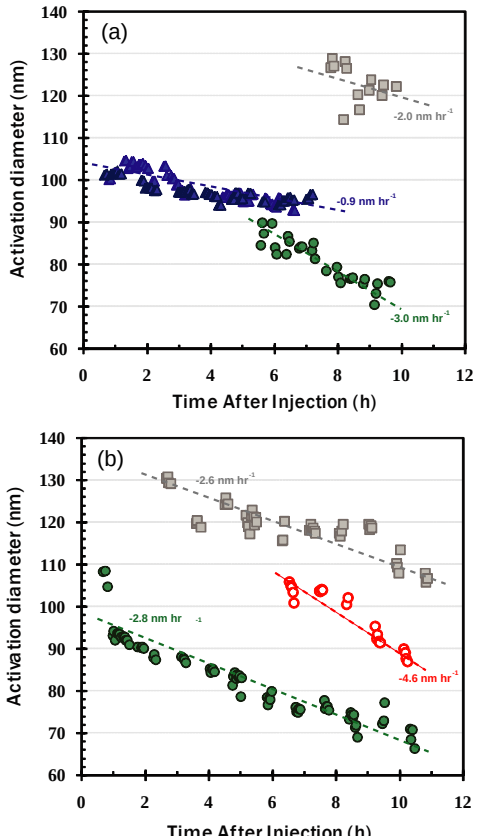

Figure 1: Activation diameter as a function of time. (a) SOA formed without OH (CFSTGC at s=0.65%: grey squares; s=1.09%: green circles), (SD at s=0.6%: blue triangles). (b) SOA formed with OH CFSTGC measurements at s=0.65% (grey squares), and s==1.09% (green circles) are shown. Open red circles correspond to aerosol passed through the thermodenuder prior to exposure to 1.09 % supersaturation in the CFSTGC.

The SD CCN counter requires 7.5 minutes per datum; to capture the impacts of aging on CCN activity, the SD is operated at 0.60% ± 0.02% supersaturation, and supplied with 100 nm diameter classified aerosol. Additional experiments were performed with the SD counter to estimate the activation diameter of the SOA. The CFSTGC is considerably faster (1 second per datum) than the SD counter, allowing for a comprehensive characterization of size resolved CCN activity using Scanning Mobility CCN Analysis (SMCA). Characterization of the size-resolved CCN activity and droplet grow for a range of supersaturations is repeated every 2.25 minutes. Changes in growth kinetics are quantified by *i*) comparison against the droplet size attained by CCN composed of pure $(NH_4)_2SO_4$, and, *ii*) using comprehensive models of the instruments to infer growth kinetic parameters of the SOA.

The water-soluble fraction of the SOA (responsible for its CCN activity) was characterized by collecting SOA on a Teflon filter and subsequently extracting the soluble part ultra-pure water. The extracted sample is subsequently atomized, dried, size selected, and characterized for its CCN activity using SMCA between 0.2 and 1.4% supersaturation (Figure 1). This

procedure is repeated for pure WSOC and mixtures with $(NH_4)_2SO_4$. Köhler Theory Analysis (KTA), combined with the CCN activity measurements, are used to infer the molecular weight, surface tension, and droplet growth kinetic characteristics of the WSOC.

We quantitatively describe the growth of activated SOA CCN by simulating the process of droplet formation within each CCN counter using comprehensive computational fluid dynamic models developed by the PI. Each of these models numerically simulates the temporal and spatial distributions of velocity, pressure, temperature and water vapor concentration throughout the growth chamber of each instrument (the particle and gas phases are coupled through release of latent heat and condensational loss of water vapor); the fields are then used to drive the condensation growth of a population of aerosol as it flows through the instrument. The kinetic model includes aerosol with size-dependant composition; condensation growth of aerosol is computed based on a size-dependant mass transfer coefficient multiplied by the difference between gas-phase and equilibrium water vapor pressure.

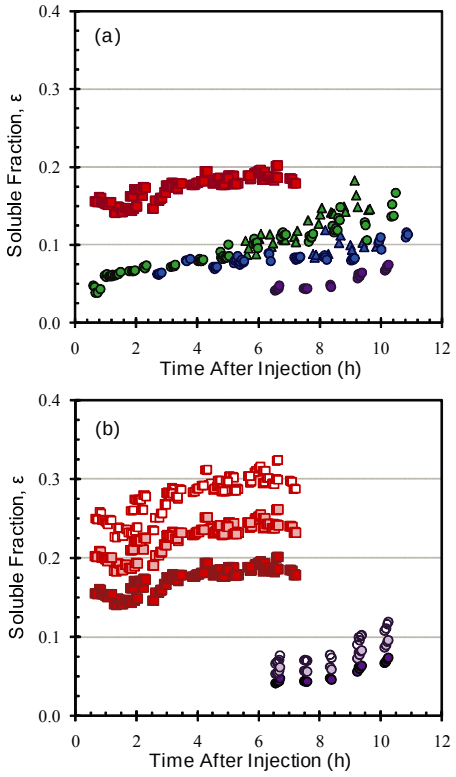

Figure 2: Inferred soluble fraction as a function of aging. Square symbols represent SD measurements; circles and triangles represent CFTGC measurements for SOA formed in the presence and absence of OH, respectively. (a) ε inferred assuming $\sigma = 66$ mN m^{-1} and $M = 156$ g mol^{-1} for SD measurements at 0.6% (red squares), CFSTGC measurements at 1.09% (green symbols), 0.65% (blue symbols), and, for aerosol passed through the thermodenuder and exposed to 1.09% supersaturation (purple symbols).

The CCN models were initialized using the appropriate geometric dimensions and operating conditions of each CCN instrument. A computational grid of 200 cells in the radial and 200 cells in the axial direction was used in each simulation; condensational growth and gravitational settling in the SD simulations commences after steady state is established for all gas-phase profiles. In CFSTGC simulations, the droplet diameter at the exit of the flow chamber is then compared against the measured size distribution, following the binning scheme used in the optical detection of the instrument. Particles with diameter larger than 2 μm are counted as droplets in the SD simulations.

Results and Discussion

In the absence of OH, the SD counter initially measures d~102 nm at s=0.6% and decreases gradually with time (Figure 1a). In the absence of OH and at s=1.09%, the CFSTGC cannot determine d within the first five hours due to insufficient CCN counts (< 10 CCN cm^{-3}). Compared to the SD, the slope of d with time in the CFSTGC is three times larger; beyond the sixth hour, the CCN activity of CFSTGC measurements (i.e., d) for both types of SOA (with and without OH) and supersaturations considered agree to within 5%. All together, SOA behavior in both instruments, suggest that hygroscopic material is volatile, and the volatility decreases with time.

To verify that aerosol volatility accounts for the differences seen in the CCN activity between instruments, we pass the most volatile SOA (i.e., formed with OH absent) through a thermodenuder before introduction into the CFSTGC. SMCA is applied to measurements at 0.65% and 1.09% supersaturation; however, the lack of CCN counts at the lower supersaturation prohibits the determination of *d* for the whole experiment. For similar reasons, the CCN activity of thermodenuded SOA at 1.09% can not be determined during the first six hours of the experiment (Figure 1b). When CCN counts are possible, *d* significantly increases (~25%) when the SOA is passed through the thermodenuder. This suggests that the non-volatile aerosol exiting the thermodenuder is less CCN-active than the semi-volatile material, and that the latter is primarily responsible for the observed CCN activity of freshly formed SOA.

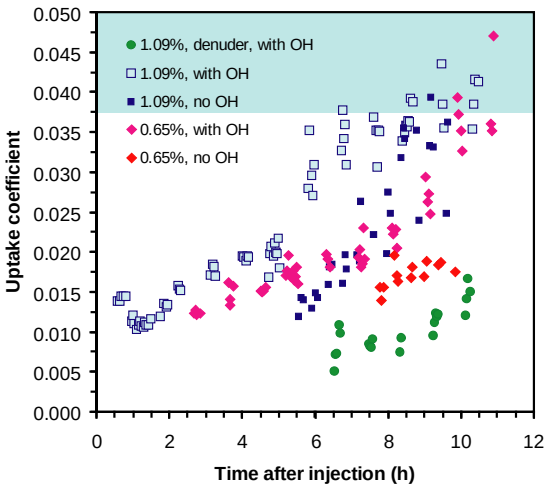

Figure 3: Inferred water vapor uptake coefficient for the growth kinetic data obtained with the CFSTGC. For comparison, the range of inferred uptake coefficient for $(NH_4)_2SO_4$ is shown in the blue shaded area.

The CCN activity of β-caryophyllene WSOC was found to be higher than in the original SOA, suggesting the WSOC comprises a small fraction of the total aerosol mass. Surprisingly, the CCN activity of WSOC from oxidation of monoterpenes and β-caryophyllene is remarkably similar, as the inferred molecular weight of the β-caryophyllene WSOC fraction was found to be 156 ±44 g mol^{-1}, versus 180 g mol^{-1} for monoterpene WSOC. Despite this, the CCN activity of monoterpene and β-caryophyllene SOA is substantially different, suggesting that the amount of WSOC in sesquiterpene SOA is much less than in monoterpene SOA. The inferred surface tension values from the salted WSOC samples suggest that it is 65±2.1 mN m^{-1}, consistent with the levels also found for monoterpene SOA.

Once the surface tension and average molar volume of the WSOC is determined, its volume fraction, ε, in the SOA can be inferred by applying Köhler Theory Analysis to the online CCN activation data (by assuming that the WSOC extracted from the filters is the same as the water-soluble material in the SOA). The result of this calculation is shown in Figure 2, where ε is plotted against time for all the experimental data of Figure 1. CCN activity is only observed when sufficient amounts (ε >0.03) of soluble non-volatile material exist in the aerosol phase. ε is minimum for aerosol processed in the thermodenuder, since that is when *d* is maximum, and is consistent with the hypothesis of WSOC volatility.

Analyzing the temporal trend of inferred ε (Figure 2) yields some very interesting aspects of the SOA aging process. Early on in the experiment (0-5 h), ε inferred from the CFSTGC 0.65% and 1.09% datasets is almost identical; this is consistent with the SOA being initially of uniform composition (and also confirms that the method to infer ε gives consistent results across a wide range of operation conditions and experiments). Later on in the experiment (5-11 h), ε between the two supersaturations diverge; the 1.09% dataset tends to infer a larger ε than for the 0.65%. This is consistent with size-dependant processing of the aerosol in the chamber; smaller particles (i.e., those with s=1.09%), because of differences in their surface-to-volume ratio, would tend to age more quickly than larger particles (i.e., those with s=0.65%).

To compare the observed droplet growth kinetics in both CCN counters, we infer the water vapor uptake coefficient *a* (a parameter that affects droplet growth rate; smaller values of *a* correspond to slower growth) from the simulations of CCN activation in each instrument, and is shown in Figure 3. Compared to the SD, growth kinetics in the CFSTGC are substantially slower, with the following characteristics: *i*) aerosol thermally treated in the thermodenuder exhibits the slowest behavior, with 4 times lower *a* than $(NH_4)_2SO_4$, *ii*) aerosol that is not pretreated in the thermodenuder exhibits slow growth kinetics early on in the experiment. Aging gradually accelerates growth, until it reaches the levels of ammonium sulfate (after 10 hours of aging), and, *iii*) the growth at s=0.65% is slower than particles with s=1.09% and takes longer to reach "sulfate rates".

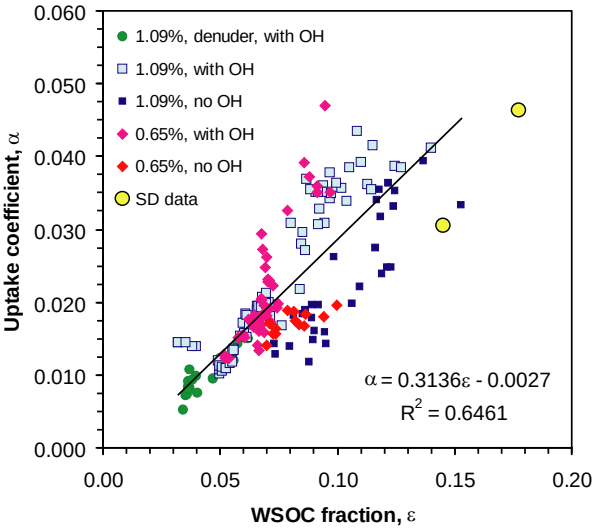

Figure 4: Inferred *a* as a function of ε for all the datasets obtained with the SD (yellow circles) and CFSTGC (all other symbols).

The diverse range of uptake coefficients inferred for CCN in both instruments may at first seem counterintuitive, but is consistent with thermal processing of the SOA in the CFSTGC and thermodenuder. Modification of CCN can happen in many ways; for example, evaporation of hygroscopic volatile compounds, preferentially from the surface layers of the aerosol, and, redistribution of insoluble "waxy" material to the CCN surface, especially if the viscosity changes substantially in the 25-35^{o}C range (i.e., it partially melts). In both cases, a "barrier" of insoluble and hydrophobic material could form between the hygroscopic fraction of the SOA, which would then decrease the growth rates of the activated CCN. The available data seems to support the thermal modification hypothesis because *i*) *a* is strongly anticorrelated with the residence time at elevated temperatures, since CCN processed in the thermodenuder exhibits the slowest growth, followed by the CFSTGC data (with non-denuded aerosol) and the SD, *ii*) CCN with s=1.09% grow more quickly in the CFSTGC than those with s=0.65%, because the WSOC fraction in the former is higher, and, *iii*) given that particles with s=1.09% have a smaller dry diameter than those with s=0.65%, the amount of insoluble material (hence the kinetic barrier) is much less; this explains why the aerosol establishes "rapid growth" kinetics towards the end of the experiment.

If volatilization of hygroscopic material (or melting of insolubles) is responsible for the variability seen in droplet growth kinetics, a common scaling law could be derived between *a* and the amount of insoluble material in the particle (i.e., ε). Indeed, this is the case (Figure 4); the correlation between the quantities is quite striking, as it shows an explicit relationship between composition and growth kinetics which applies for all the experiments and CCN instruments used in the study.

In summary, numerous important findings came out of this study. First, the hygroscopic material in the SOA is semivolatile. The implications for CCN measurements are very important; the temperature at which CCN measurements are carried out, if the aerosol is volatile and composed of a low fraction of soluble material, may strongly bias the observed CCN activity. In our study, this bias shifted measured activation diameters between 25 and 30% and prevented CCN detection during the first half of the experiments. However, the bias can be identified and quantified if the aerosol is periodically passed through a thermodenuder, or, if CCN measurements are undertaken at different temperatures. The volatility of WSOC carries important

implications for atmospheric processes; since the temperature range in our measurements is typical of diurnal variations found during summertime conditions (where biogenic emissions and photochemical activity, hence SOA production, are maximum), volatilization of small amounts of aerosol may induce an unanticipated diurnal cycle of CCN activity.

Another major finding of this study is that the less volatile material in sesquiterpene SOA is not very hygroscopic, but can impact droplet growth kinetics. The degree of kinetic limitations depend on the volume fraction of insoluble material in the SOA, as heating of the aerosol tends to decrease the droplet growth rates of the CCN. We postulate this to be result of soluble material evaporating from the surface of the SOA, potentially combined with redistribution (by melting) of "waxy" material to the CCN surface; both mechanisms would create a kinetic barrier that partially impedes water vapor condensation. An explicit relationship between the water vapor uptake coefficient (used here to represent variations in droplet growth kinetics) and WSOC fraction implies that one mechanism (that scales inversely with soluble volume fraction) is likely responsible for the observed growth delay, and, that it is from the presence of insoluble material. The implications of these findings for cloud droplet formation are many: *i*) similar to CCN activity, a diurnal cycle of growth kinetics for biogenic aerosol may exist, with profound impacts on the droplet size distribution and aerosol-cloud interactions, *ii*) the concept of "external mixing"' may not be only important for CCN activity (i.e., *s*), but also for droplet growth kinetics, *iii*) evaporation of SOA in the dry, free troposphere could form particles that are kinetically limited, and, *iv*) SOA with high soluble fractions (e.g., monoterpene SOA) may grow as quickly as inorganic salt CCN (e.g., $(NH_4)_2SO_4$) (which is consistent with the limited data available to date (Engelhart et al., in review). Whether a simple relationship between a and ε exists in other SOA systems still remains to be found, but the approach outlined in this study could be used to unravel and parameterize the complex relationship between volatility, CCN activity, growth kinetics and composition.

PARTICIPATION IN FIELD CAMPAIGNS.

Together with funding from numerous other US and European sources, the PI during the 2007-2008 period has deployed CCN instrumentation to characterize the cloud droplet formation potential of aerosol through many areas of the globe. Specifically, data were collected from the following campaigns:

- **TexAQS/GoMACCs**. (http://nenes.eas.gatech.edu/FieldPhotos/GoMACCs/Page.html) CCN measurements were obtained aboard the CIRPAS Twin Otter and NOAA WB-P3 during research flights (based out of Houston, TX) from July-October, 2006. Experimental data was collected for eleven of the thirteen scheduled flight missions. Specifically, CCN number was measured as a function of supersaturation (ranging from 0.1 to 0.4%) for 1-second intervals during each flight. In this study we evaluate our ability to predict CCN number and compare the values to measurements from ten flight days. In addition we observe changes in CCN downwind of power plant plumes (e.g., Parish power plant) and sources heavily influenced by industrial (petrochemical industry) and urban (houston) sources. This work is being prepared for submission.Partial funding for this project were provided by NOAA and NSF.

- **MASE-II**. (http://nenes.eas.gatech.edu/FieldPhotos/MASEII/Page.html) CCN measurements using SMCA (and other size-resolved methodologies) were obtained aboard the CIRPAS Twin Otter during research flights (based out of Monterey, CA) during July, 2008. Partial funding for this project were provided by NOAA and NSF.

The PI and his research group are currently analyzing the data from all these sources, placing an emphasis on the role of organics and aerosol mixing state on droplet growth kinetics and CCN activity. In addition to in-situ CCN measurements,

evaporated cloud water residual samples (collected from a Counterflow Virtual Impactor) were collected to characterize the thermodynamic properties of the WSOC. Samples were collected for three different levels within the cloud (top, middle, and bottom) to obtain a comprehensive characterization of the water-soluble organics (and their evolution) within clouds. These results are in preparation for submission.

Additional research supported by this proposal

EFFECT OF SOLUTE DISSOLUTION KINETICS ON CLOUD DROPLET FORMATION: EXTENDED KÖHLER THEORY

A common assumption for partially soluble compounds is that solute instantaneously dissolves and distributes uniformly throughout the droplet. Compared to electrolytes, the majority of organic compounds are not very soluble in water, do not deliquesce, have a higher molar mass and thus diffuse more slowly in aqueous solutions. The implication for a growing droplet is that mass transfer of the dissolving organics may not be fast enough to assure uniform distribution of solute through the droplet volume; this kinetic limitation may decrease the solute concentration at the droplet surface and increase the droplet equilibrium vapor pressure. This study focuses on exploring the effects of solute dissolution kinetics on cloud droplet formation. A numerical model is developed to simulate the dissolution of solute from a solid core located at the center of the droplet and its diffusion throughout the aqueous phase of the growing drop. The numerical simulations are parameterized and introduced into Köhler theory for a thorough analysis of dissolution kinetics on CCN activity.

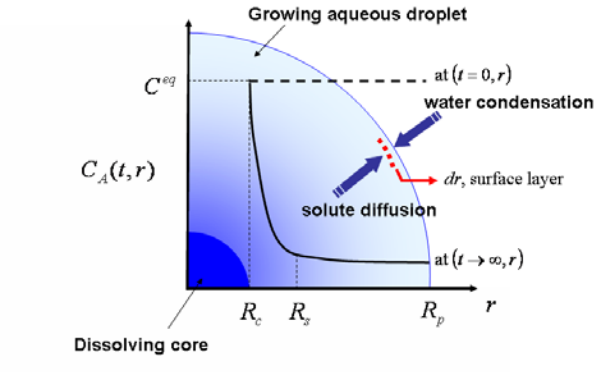

Figure 5: Illustration of the problem geometry and the solute concentration profile. R_s represents the location where the concentration gradient becomes effectively zero.

Dissolution kinetics model

The numerical model is based on conservation of mass for the dissolving substance in a spherically symmetric droplet (Figure 5). The solute originates from a spherical solid core located at the center of the droplet; after dissolution, we assume that the solute mass transport occurs (via molecular diffusion) from the core to the droplet surface. Assuming that the solid core is composed of a slightly soluble substance *A*, the dissolution and transport of solute from the core into the droplet aqueous phase can be described by,

$$\frac{\partial C_A(t,r)}{\partial t} = D_{Aw}\left[\frac{1}{r^2}\frac{\partial}{\partial r}\left(r^2\frac{\partial C_A(t,r)}{\partial r}\right)\right] \qquad (1)$$

where $C_A(t,r)$ denotes the concentration of *A* at time *t* and distance *r* from the core droplet center, and D_{Aw} is the diffusivity of *A* in water. D_{Aw} depends on temperature and solute molecular size, but typically ranges between 10^{-9} and 10^{-10} m^2s^{-1}. The concentration of *A* throughout the droplet volume is initially equal to its solubility in water, $C_A(0,r)=C^{eq}$, while the solution is saturated with *A* at the core-solution interface, located at $r = R_c$, $C_A(t>0,R_c)=C^{eq}$. The boundary condition at

the droplet surface is somewhat more complex, as solute diffusion and water condensation affect the surface concentration of *A*. It can be shown, however, that at the droplet surface,

$$\frac{\partial C_A(t,R_p)}{\partial t} = \frac{-3}{D_p}\left[C_A(t,R_p)\frac{dD_p}{dt} + 4D_{Aw}\frac{\partial C_A(t,R_p)}{\partial D_p} \right] \tag{2}$$

$\frac{dD_p}{dt}$ can be approximated in terms of the ambient conditions, as

$$\frac{dD_p}{dt} \approx \frac{1}{G}\frac{S-1}{D_p} = \frac{1}{G}\frac{s}{D_p} \tag{3}$$

where $s = S - 1$ is the ambient water vapor supersaturation, and *G* is a kinetic growth parameter. Substitution of Equation (3) into Equation (2) gives,

$$\frac{\partial C_A(t,R_p)}{\partial t} = \frac{-3}{D_p}\left[\frac{1}{G}\frac{sC_A(t,R_p)}{D_p} + 4D_{Aw}\frac{\partial C_A(t,R_p)}{\partial D_p} \right] \tag{4}$$

Equation (4) is the droplet surface boundary condition used to integrate Equation (1).

Including dissolution kinetics into Köhler theory

It is desirable to introduce appropriate modifications to Köhler theory when assessing the effects of solute mass transfer kinetics on cloud droplet formation. This could be accomplished by establishing a relationship between the concentration of solute at the droplet surface, C^*, and the dissolution kinetics parameters D_{Aw}, s, $D_{p..}$ Assuming that the concentration at the droplet interface is a pseudo-steady state (i.e., the left hand side of Equation (4) is zero), it can be shown that C^* follows the following form,

$$C^* = \frac{C^{eq}}{1 + k\frac{\omega s}{4GD_{AB}}} \tag{5}$$

Where ω is the ratio of droplet to core size. Equation (5) describes the solute surface concentration at the droplet surface in terms of solubility, ambient supersaturation, solute diffusivity, droplet and core size, and the non-dimensional coefficient *k* which is related to the mass transfer kinetics. Fitting Equation 5 to numerical integrations (at steady state) yield k=0.8 with an error of 10%. Solute transport kinetics is introduced in Köhler Theory by introducing Equation (5) into "classical" theory for a CCN containing partially-soluble salt (Asa-Awuku and Nenes, 2007),

$$s_{eq} = \frac{4M_w\sigma_w}{RT\rho_w D_p} - \frac{6n_s M_w \upsilon_s}{\pi\rho_w D_p{}^3} - \frac{M_w}{\rho_w}\upsilon_{ss}\frac{C^{eq}}{1 + 0.8\frac{\omega(s - s_{eq})}{4GD_{AB}}} \tag{6}$$

When applying Equation (6), the undissolved core diameter (or radius) needs to be computed. This can be done from the solute mass balance, provided that the number of moles of partially-soluble salt, n_{ss}^{tot}, is known. Assuming that the core is composed exclusively of slightly soluble material, R_c is calculated from a mass balance,

$$R_c = \left\{ \frac{3}{4\pi} \frac{M_{ss}}{\rho_{ss}} \left(n_{ss}^{tot} - n_{ss} \right) \right\}^{1/3} = \left\{ \frac{3}{4\pi} \frac{M_{ss}}{\rho_{ss}} \left(n_{ss}^{tot} - 4\pi \int_{R_c}^{R_p} r^2 C_{ss}(t,r) dr \right) \right\}^{1/3} \quad (7)$$

where n_{ss} is the amount of dissolved solute, M_{ss}, ρ_{ss} are the slightly soluble molar mass and density, respectively. In calculating n_{ss}, the steady-state concentration profile $C_{ss}(t,r)$ is given by,

$$C_{ss}(t,r) = \frac{\left(C^* - C^{eq} \right) R_p}{\left(R_c - R_p \right)} \left[\frac{R_c}{r} + 1 \right] + C^{eq} \quad (8)$$

Substitution of Equation (8) into (7) and integration yields an algebraic equation that is numerically solved for R_c.

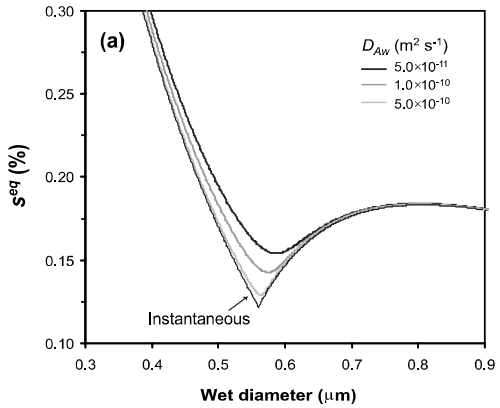

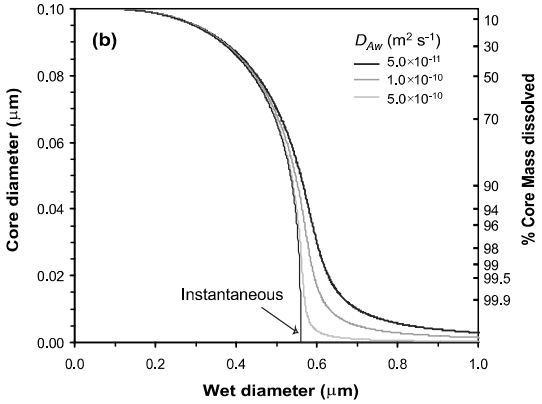

Figure 6: Köhler curves modified to include the effect of solute dissolution kinetics. The CCN dry diameter is 100 nm and composed of a partially soluble substance with 1750 kg m^{-3} density, 0.132 kg mol^{-1} molar mass, van't Hoff factor of 2 and a solubility of 10^{-2} kg kg^{-1}. Ambient supersaturation is assumed to be 1.0%. Calculations are presented as (a) s_{eq} vs. wet diameter for a range of D_{Aw}, and, (b) amount of partially soluble core left, expressed in terms of its diameter and % mass dissolved.

Effect of dissolution kinetics on equilibrium supersaturation

Figure 6 displays Köhler curves with and without the effect of solute dissolution kinetics. In these calculations, the dry CCN is 100 nm in diameter and composed of a partially soluble substance with 1750 kg m^{-3} density, 0.132 kg mol^{-1} molar mass (similar to that of glutaric acid), van't Hoff factor of 2 and a solubility of 10^{-2} kg kg^{-1}. Ambient supersaturation is assumed to be 1.0%. Assuming that dissolution and mass transfer of the solute is instantaneous (blue curves) yields a "typical" Köhler curve (Figure 6a). At small wet diameters, the amount of liquid water is insufficient to completely dissolve the core, hence the concentration of solute is constant throughout the droplet volume until complete dissolution (here at ~0.56 μm).

For larger wet diameters, the droplet dilutes as it grows and develops the characteristic "Köhler" maximum in s_{eq}. When dissolution kinetics are considered, the decrease in C^* (Equation 9) "shifts" s_{eq} to higher levels at small wet diameters; this effect is negligible for large solute diffusivity (> 5×10^{-10} m^2 s^{-1}) but becomes modest for low diffusivity (< 2.5×10^{-10} m^2 s^{-1}). Here, the effect on s_{eq} can be ~10% for $D_A = 5\times10^{-10}$ m^2 s^{-1}, but as large as 70% for smaller values of the coefficient. The effect of dissolution kinetics is also clearly seen on the core diameter and amount of dissolved solute (Figure 6b); as dissolution kinetics require a finite time to redistribute soluble material throughout the droplet volume, core is present for a wider range of wet diameters and thus can even influence the region beyond the "traditional" critical diameter. For example, at 0.56 μm wet diameter the core is practically dissolved for instantaneous to large solute diffusivity (>5×10^{-10} m^2 s^{-1}), while only 70% (i.e., a core more

than half its dry size) is dissolved at lower diffusivity. Thus, appreciable amounts of core can be present at droplet sizes between 0.5 and 1 micron; conditions can be found for which core is seen at even larger sizes (not shown).

In addition to the shape of the Köhler curve, dissolution kinetics may also impact the critical supersaturation (i.e., its global maximum), especially when the CCN contains small amounts of soluble salts. This is shown in Figure 7, which displays Köhler curves with (solid lines) and without (shaded lines) the effect of solute dissolution kinetics; the CCN considered have a dry diameter of 100 nm and are composed of a mixture of NH_4HSO_4 and a partially soluble substance with the properties of Figure 6. Ambient supersaturation, s, is assumed to be 1.0%, and D_{Aw} = 7.5×10^{-11} m^2 s^{-1}. When the sulfate mass fraction ranges between 0.05 and 0.1, the critical supersaturation, s_c, of the CCN increases substantially, between 2 and 5%. For higher sulfate mass fractions, s_c increases are negligible. This behavior can be explained by comparing the concentration of salt and slightly soluble substance around the critical diameter, D_{crit}. If there is very little sulfate present, then D_{crit} is close to the particle dry diameter, so dissolution kinetics have a minor effect on s_c; when there is significant amounts of sulfate, the slightly soluble compound (and its concentration variations thereof from dissolution kinetics) does not significantly impact the Raoult term of the Köhler curve. Only when both components yield comparable concentrations about the D_{crit}, can concentration variations from dissolution kinetics have an appreciable impact on the equilibrium vapor pressure. It should be noted that even when s_c is not affected, the shape of the Köhler curve (hence the droplet growth kinetics) may substantially change if dissolution kinetics are slow enough (Figure 7).

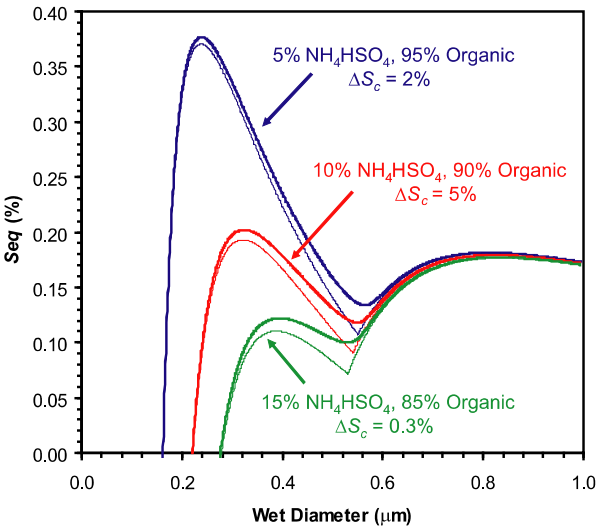

Figure 7: Köhler curves with (solid lines) and without (shaded lines) the effect of solute dissolution kinetics. The CCN have 100 nm dry diameter and are a mixture of NH_4HSO_4 and a partially soluble substance with the same properties as in Figure 6. Ambient supersaturation is assumed to be 1.0%, and D_{Aw} =7.5×10^{-11} m^2 s^{-1}.

Based on our analysis, compounds with $D_{Aw} > 5\times10^{-10}$ m^2 s^{-1} will not experience significant changes in the Köhler curve from mass transfer kinetics. This is consistent with the finding that CCN composed of soluble electrolytes and low molecular weight organics tend to follow Köhler theory; although deliquesced aerosol do not have a solute "core" during droplet activation, our analysis still applies, since the region about the center of the droplet can be much more concentrated with solute and virtually as a "core". However, for higher molecular weight compounds (e.g., HULIS) and low temperatures, where diffusivity is low (i.e., $D_{Aw} \leq 2.5\times10^{-10}$ m^2 s^{-1} and below), mass transfer kinetics may impact equilibrium vapor pressure; this can contribute to the discrepancy often reported between theoretical predictions (i.e., underestimation of s_c) and observations of CCN activity and growth kinetics. In terms of laboratory experiments, dissolution & mass transfer kinetics may also in part explain why activation curves for organic CCN (i.e., measurements of the ratio between activated CCN and total condensation nuclei as a function of particle size) tend to be broader than for inorganic and low molecular weight CCN. In terms of ambient CCN, solute dissolution kinetics may not affect s_c if the CCN contains substantial amounts of inorganic electrolytes and low molecular weight organic acids. Conversely, solute dissolution kinetics may influence droplet formation when (a) a partially soluble core is present during the CCN activation, and, (b) the partially soluble solute constitutes a significant fraction of the total solute. In the atmosphere, such particles could correspond to biogenic and secondary organic

aerosol. If slow enough, dissolution kinetics may also help explain why CCN and cloud droplet number closure studies for ambient aerosol suggest that organics behave as "insoluble"; even if soluble, dissolved organics may diffuse too slowly to fully affect the CCN vapor pressure, hence appearing less "soluble" than they really are. Dissolution kinetics become more important with increasing supersaturation and low temperatures, hence their effects are expected to be most prominent for supercooled droplets, pristine stratocumulus and convective clouds.

The results are cited as follows:

Asa-Awuku, A., and Nenes, A. (2007) The Effect of Solute Dissolution Kinetics on Cloud Droplet Formation: Extended Köhler theory, J.Geoph.Res., 112, D22201, doi:10.1029/2005JD006934

Conclusion

Over the past three years, several exciting and insightful developments and deliverables have resulted from the aid of the NASA ESS funding. The PI and fellowship recipient gratefully thank the NASA ESS program for sponsoring the research towards the completion of her doctoral thesis.

References

1. Cachier, H., et al., *Particulate Content Of Savanna Fire Emissions.* Journal Of Atmospheric Chemistry, 1995. **22**(1-2): p. 123-148.
2. Yamasoe, M.A., et al., *Chemical composition of aerosol particles from direct emissions of vegetation fires in the Amazon Basin: water-soluble species and trace elements.* Atmospheric Environment, 2000. **34**(10): p. 1641-1653.
3. Andreae, M.O. and P.J. Crutzen, *Atmospheric aerosols: Biogeochemical sources and role in atmospheric chemistry.* Science, 1997. **276**(5315): p. 1052-1058.
4. Shulman, M.L., et al., *Dissolution behavior and surface tension effects of organic compounds in nucleating cloud droplets.* Geophysical Research Letters, 1996. **23**(3): p. 277-280.
5. Decesari, S., et al., *Solubility properties of surfactants in atmospheric aerosol and cloud/fog water samples.* Journal Of Geophysical Research-Atmospheres, 2003. **108**(D21): p. 4685.
6. Saxena, P. and L.M. Hildemann, *Water-soluble organics in atmospheric particles: A critical review of the literature and application of thermodynamics to identify candidate compounds.* Journal Of Atmospheric Chemistry, 1996. **24**(1): p. 57-109.
7. Mayol-Bracero, O.L., et al., *Water-soluble organic compounds in biomass burning aerosols over Amazonia - 2. Apportionment of the chemical composition and importance of the polyacidic fraction.* Journal Of Geophysical Research-Atmospheres, 2002. **107**(D20): p. 8091.
8. Kiss, G., E. Tombacz, and H.C. Hansson, *Surface tension effects of humic-like substances in the aqueous extract of tropospheric fine aerosol.* Journal Of Atmospheric Chemistry, 2005. **50**(3): p. 279-294.
9. Decesari, S., et al., *Characterization of water-soluble organic compounds in atmospheric aerosol: A new approach.* Journal Of Geophysical Research-Atmospheres, 2000. **105**(D1): p. 1481-1489.
10. Krivacsy, Z., et al., *Study of humic-like substances in fog and interstitial aerosol by size-exclusion chromatography and capillary electrophoresis.* Atmospheric Environment, 2000. **34**(25): p. 4273-4281.
11. Graham, B., et al., *Water-soluble organic compounds in biomass burning aerosols over Amazonia - 1. Characterization by NMR and GC-MS.* Journal Of Geophysical Research-Atmospheres, 2002. **107**(D20).
12. Facchini, M.C., et al., *Surface tension of atmospheric wet aerosol and cloud/fog droplets in relation to their organic carbon content and chemical composition.* Atmospheric Environment, 2000. **34**(28): p. 4853-4857.
13. Havers, N., et al., *Spectroscopic characterization of humic-like substances in airborne particulate matter.* Journal Of Atmospheric Chemistry, 1998. **29**(1): p. 45-54.

14. Guenther, A., et al., *A Global-Model of Natural Volatile Organic-Compound Emissions.* Journal of Geophysical Research-Atmospheres, 1995. **100**(D5): p. 8873-8892.
15. Guenther, A., et al., *Biogenic hydrocarbon emissions and landcover/climate change in a subtropical savanna.* Physics and Chemistry of the Earth Part B-Hydrology Oceans and Atmosphere, 1999. **24**(6): p. 659-667.
16. Guenther, A., et al., *Natural emissions of non-methane volatile organic compounds; carbon monoxide, and oxides of nitrogen from North America.* Atmospheric Environment, 2000. **34**(12-14): p. 2205-2230.
17. Kanakidou, M., et al., *Organic aerosol and global climate modelling: a review.* Atmospheric Chemistry And Physics, 2005. **5**: p. 1053-1123.
18. Seinfeld, J.H. and J.F. Pankow, *Organic atmospheric particulate material.* Annual Review of Physical Chemistry, 2003. **54**: p. 121-140.
19. Claeys, M., et al., *Formation of secondary organic aerosols from isoprene and its gas-phase oxidation products through reaction with hydrogen peroxide.* Atmospheric Environment, 2004. **38**(25): p. 4093-4098.
20. Gao, S., et al., *Low-molecular-weight and oligomeric components in secondary organic aerosol from the ozonolysis of cycloalkenes and alpha-pinene.* Journal of Physical Chemistry A, 2004. **108**: p. 10147-10164.
21. Huff-Hartz, K.E., et al., *Cloud condensation nuclei activation of monoterpene and sesquiterpene secondary organic aerosol.* Journal of Geophysical Research-Atmospheres, 2005. **110**(D14): p. D14208.
22. Varutbangkul, V., et al., *Hygroscopicity of secondary organic aerosols formed by oxidation of cycloalkenes, monoterpenes, sesquiterpenes, and related compounds.* Atmospheric Chemistry and Physics, 2006. **6**: p. 2367-2388.
23. Aschmann, S.M., R. Atkinson, and J. Arey, *Products of reaction of OH radicals with alpha-pinene.* Journal of Geophysical Research-Atmospheres, 2002. **107**(D14): p. 4191.
24. Alfarra, M.R., et al., *A mass spectrometric study of secondary organic aerosols formed from the photooxidation of anthropogenic and biogenic precursors in a reaction chamber.* Atmospheric Chemistry and Physics, 2006. **6**: p. 5279-5293.
25. Forstner, H.J.L., R.C. Flagan, and J.H. Seinfeld, *Secondary organic aerosol from the photooxidation of aromatic hydrocarbons: Molecular composition.* Environmental Science & Technology, 1997. **31**(5): p. 1345-1358.
26. Hamilton, J.F., et al., *Investigating the composition of organic aerosol resulting from cyclohexene ozonolysis: low molecular weight and heterogeneous reaction products.* Atmospheric Chemistry and Physics, 2006. **6**: p. 4973-4984.
27. Kalberer, M., M. Sax, and V. Samburova, *Molecular size evolution of oligomers in organic aerosols collected in urban atmospheres and generated in a smog chamber.* Environmental Science & Technology, 2006. **40**(19): p. 5917-5922.
28. Dommen, J., et al., *Laboratory observation of oligomers in the aerosol from isoprene/NOx photooxidation.* Geophysical Research Letters, 2006. **33**(13): p. L13805.
29. Kroll, J.H., et al., *Secondary organic aerosol formation from isoprene photooxidation.* Environmental Science & Technology, 2006. **40**(6): p. 1869-1877.
30. Baltensperger, U., et al., *Secondary organic aerosols from anthropogenic and biogenic precursors.* Faraday Discussions, 2005. **130**: p. 265-278.
31. Limbeck, A., M. Kulmala, and H. Puxbaum, *Secondary organic aerosol formation in the atmosphere via heterogeneous reaction of gaseous isoprene on acidic particles.* Geophysical Research Letters, 2003. **30**(19): p. 1996.
32. Rogge, W.F., et al., *Quantification of Urban Organic Aerosols at a Molecular-Level - Identification, Abundance and Seasonal-Variation.* Atmospheric Environment Part a-General Topics, 1993. **27**(8): p. 1309-1330.
33. Seinfeld, J.H. and S.N. Pandis, *Atmospheric Chemistry & Physics: From Air Pollution to Climate Change*. 1998: